Earth-to-Moon Low Energy Transfers Targeting L_1 Hyperbolic Transit Orbits

Francesco Topputo
Massimiliano Vasile
Franco Bernelli-Zazzera

Aerospace Engineering Department, Politecnico di Milano
Via La Masa, 34 - 20156, Milan, Italy
{topputo,vasile,bernelli}@aero.polimi.it

New Trends in Astrodynamics and Applications II
Princeton University, Princeton, NJ, 3–5 June 2005

Abstract

In the frame of the lunar exploration, numerous future space missions will require the maximization of the payload mass, while simultaneously achieving reasonable transfer times. To fulfil this request, low energy non-Keplerian orbits could be used to reach the Moon instead of common high energetic transfers. The low energy solutions can be split into two main categories depending on the nature of the trajectory approaching the Moon: the low energy transit orbits, approaching the Moon from the interior equilibrium point L_1 and the Weak Stability Boundary transfers, reaching the Moon after passing through L_2.

This paper proposes an alternative way to exploit the opportunities offered by the L_1 transit orbits for the design of Earth-Moon transfers. First, in a neighborhood of the L_1 point, the three-body dynamics is linearized and written in normal form; then the whole family of nonlinear transit orbits is obtained by selecting the appropriate non-trivial amplitudes associated to the hyperbolic part. The L_1-Earth arc is close to a 5:2 resonant orbit with the Moon, whose perturbations cause the apogee raising. In a second step, two selected low altitude parking orbits around the Earth and the Moon are linked with the transit orbit by means of two three-body Lambert's arcs, solutions of two two-point boundary value problems.

The resulting Earth-to-Moon trajectories prove to be very efficient in the Moon captured arc and allow to save approximately 100 m/s in Δv cost if compared to the Hohmann transfer.

1 Introduction

The patched conic method transfer represents the classical technique adopted to design interplanetary and lunar transfers. In the case of a journey to the Moon, a Hohmann transfer takes typically a few days and requires a Δv cost which depends on the altitudes of the initial Earth and final Moon orbit. For instance, the cost required to go from a circular Earth parking orbit with altitude $h_E = 167\ km$ to a $h_M = 100\ km$ circular orbit around the Moon is equal to $\Delta v_H = 3991\ m/s$ and the time of flight is $\Delta t_H = 5\ days$ [1]. The Hohmann path is obtained by patching together two different conic arcs, defined within two two-body problems, and just one gravitational attraction is considered acting on each leg. As a consequence, this formulation involves a hyperbolic excess velocity relative to the Moon which determines the size of the Δv maneuver required to put the spacecraft into a stable final Moon orbit. When shorter times are required, as in the Apollo figure 8 trajectory, even more expensive solutions must be taken into account.

In the past several authors have faced the problem of finding Δv-efficient solutions aimed at reducing the cost associated to a lunar transfer; however, the results obtained so far are difficult to compare directly since the Δv cost is a function of the departure and arrival orbits radii. Anyway, the general idea has been to widen the dynamical model involving two or more gravitational attractions simultaneously acting on the spacecraft. Only in this broader context, in fact, some new dynamical behaviors, provided by the chaotic regime, can be exploited to improve the performances of the transfer trajectories. Some researches were carried out in order to find multi-impulse transfers in the frame of the restricted three- and four-body models [2, 3]. Such studies, nevertheless, dealt just with the optimization problems and did not underline the potentiality of the new dynamical models.

One of the most important step forward in the n-body mission design was due to Belbruno [1] who, exploiting the intrinsic nature of the Sun-Earth-Moon dynamics, devised a method to obtain Earth-to-Moon transfer trajectories with no hyperbolic excess velocity at Moon arrival. The so called Belbruno's trajectories were based on the concept of *Weak Stability Boundaries* (WSB), which are regions in the phase space where the gravitational attractions of the Sun, Earth and Mood tend to balance.

The idea, briefly described here, was to depart from a given point near the Earth and fly-by the Moon to gain enough energy to go at a distance of approximately four Earth-Moon length units ($1.5 \cdot 10^6\ km$). In this region, due to the high sensitivity to initial conditions, a small Δv was used to put the spacecraft into a lunar captured trajectory that led to an unstable ellipse, where another maneuver was performed to put the spacecraft into a lunar circular orbit (figure 1). Such a new technique showed to be more economical than the Hohmann transfer although the time of flight was on the order of 3-5 months. As a result, a WSB transfer between the two circular orbits mentioned above ($h_E = 167\ km$ and $h_M = 100\ km$) has a total cost of $\Delta v = 3838\ m/s$ which is 153 m/s less than the Hohmann transfer cost.

One decade later, Koon et al [4] applied dynamical system theory to analyze the WSB transfers and gave an alternative explanation of the Moon's capture mechanism found by Belbruno. Using two coupled planar circular Restricted Three-Body Problems (R3BPs), they showed that the full WSB trajectory could be separated

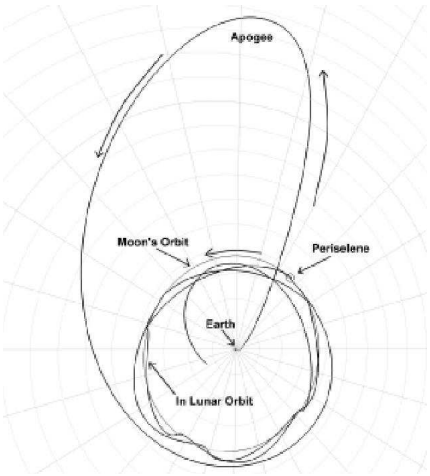

Figure 1: A typical WSB trajectory [1].

into two "deterministic" legs: the first is a piece of the unstable manifold of a L_2 Lyapunov orbit in the Sun-Earth system, while the second, the one that allows the Moon's capture, is a leg of the stable manifold associated to a L_2 Lyapunov orbit in the Earth-Moon system. When these two manifolds intersect in the configuration space, a small Δv maneuver performs the step from the first manifold to the second.

The studies above deal with the problem of transferring a spacecraft from an Earth parking orbit to an orbit about the Moon by taking into account the gravitational attractions of the Sun, Earth and Moon. In a WSB trajectory, the action of the Sun is relevant because, during the transfer, the spacecraft is far from both the Moon and the Earth. Looking for a *direct* Earth-to-Moon transfer, the Earth-Moon-Spacecraft R3BP may be considered. Trajectories could be later refined in more precise models including secondary effects like the orbital eccentricity and fourth-body perturbations. Furthermore, the smallest energy level that allows the transfer corresponds to the Jacobi constant at $L1$ (C_1), which is lower than the level of a WSB trajectory. In a WSB transfer, indeed, the Moon is approached from the far side, so the minimum energy needed to open the outer Hill's curves is the Jacobi constant at L_2 (C_2). In the Earth-Moon system the transfer is direct, through L_1, so the minimum energy value is C_1 that is higher (i.e. lower energy) than C_2.

The studies on the L_1 transit orbits date back to work of Conley [5] who first proposed to apply such solutions. In particular, Conley suggested to link the L_1 transit orbits with two "looping" orbits, around the Earth and the Moon, by means of an impulse given at the crossing point. His idea was to approximate the motion of the spacecraft with the linearized equations of the R3BP in the neighborhood of L_1, and with those of the two-body problem in the neighborhood of the primaries. In this way, a slightly more sophisticated version of the patched conic method was formulated.

Sweetser [6] quantified the minimum Δv needed to reach the Moon from the Earth by transiting through L_1. This minimum was established by analyzing the variation of the Jacobi constant but, unfortunately, the corresponding minimum-Δv trajectory was not found. Pernicka et al [7] were able to find a transfer trajectory close to this one. Their solution links a $h_E = 167\ km$ Earth orbit with a $h_M =$

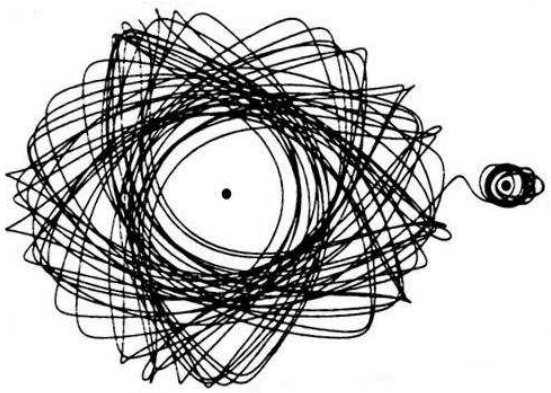

Figure 2: The Earth-Moon transfer found from Bolt and Meiss [10].

100 km Moon orbit requiring $\Delta v = 3824\ m/s$ and $\Delta t = 292\ days$ while the minimum theoretical cost for such a transfer is equal to $\Delta v_{th} = 3726\ m/s$. Very recently, Mengali and Quarta [8] have computed a family of optimal bi-impulse solutions, linking the same orbits, which transit above the L_1 point and whose best result requires $\Delta v = 3861\ m/s$ but it is only $\Delta t = 85\ days$ long. Yagasaki [9] analyzed the behavior of such solutions when solar perturbation is taken into account and found that a sensitive reduction of the total cost can be achieved in this enlarged model.

Another approach to the design of low energy transfers through L_1 aims at guiding the spacecraft from an initial state to a desired final state by using a carefully chosen sequence of small perturbations; this process is called *targeting*. Bolt and Meiss [10] applied the targeting to find short orbits in the planar Earth-Moon-Spacecraft R3BP. They were able to find a low energy transfer between two $h_E = 53291\ km$ and $h_M = 12232\ km$ very high altitude orbits (figure 2). The time of flight was equal to $\Delta t = 748\ days$ (i.e. 2.05 $years$) while the overall Δv required by this transfer was 750 m/s meaning that such solution requires 38% less Δv than the analogous Hohmann transfer which is 1220 m/s. Nevertheless, this transfer has two weak key features. First, the altitudes of the departure and arrival orbits are chosen within the chaotic regions. Such method, indeed, uses the highly nonlinear dynamics while the phase space around the primaries is characterized by an ordered dynamics. Second, the high time of flight makes not worth the savings.

In order to reduce the transfer times, another approach was suggested by Schroer and Ott [11] who applied a modified targeting procedure and found short orbits that "quickly" lead to the Moon. Through this method they were able to find a transfer between the same departure and arrival orbits used by Bolt and Meiss with a time of flight equal to $\Delta t = 377.5\ days$ while requiring the same Δv. Assuming again the same two orbits, Macau [12] found a transfer involving a cost slightly higher ($\Delta v = 767\ m/s$) than the two previous works, but with a considerable shorter transfer time equal to $\Delta t = 284\ days$. Ross [13] analyzed the same problem and found a family of solutions with the best one requiring a Δv equal to 860 m/s and a transfer time of only $\Delta t = 65\ days$.

The present study analyzes the nature of the low-energy transfers to the Moon. The trajectories presented here differ from the usual conic paths to the Moon be-

cause they are defined in the R3BP. They differ also from the WSB transfers since the approach undertaken here aims to directly, through L_1, reach the Moon by flying on orbits *shadowing* the L_1 stable manifold. First, the analysis of the linearized dynamics in the neighborhood of the L_1 point leads to a parameterization of the family of L_1 linear transit orbits useful for a low energy lunar transfer. In analogy with the generation of the invariant manifolds [4], the initial condition obtained by the linear analysis is propagated under the full original nonlinear system. This process is used to define the L_1 nonlinear transit orbits. Since these orbits do not approach the Earth in a short time, additional maneuvers, as suggested by Conley, are introduced to link them with low altitude Earth and Moon orbits.

The L_1-Moon arc is defined by linking nonlinear transit orbits with low altitude Moon orbits by means of a Lambert's three-body arc obtained by solving a Two-Point Boundary Value Problem (2PBVP) within the R3BP dynamics. On the other hand, the L_1-Earth arc is first perturbed by means of n small Δv maneuvers and then linked with the low altitude Earth orbit using another Lambert's three-body arc. The problem so stated has been optimized and the results found are compared with the classical Hohmann one.

2 Dynamics

Differential equations, describing the motion of a negligible mass under the gravitational attraction of two primaries, are written in a synodic reference frame (figure 3) and are the well-known [4]

$$\begin{cases} \ddot{X} - 2\dot{Y} &= \Omega_X \\ \ddot{Y} + 2\dot{X} &= \Omega_Y \\ \ddot{Z} &= \Omega_Z \end{cases} \tag{1}$$

where the subscripts denote the partial derivatives of the function

$$\Omega(X,Y,Z) = \frac{1}{2}(X^2+Y^2) + \frac{1-\mu}{R_1} + \frac{\mu}{R_2} + \frac{1}{2}\mu(1-\mu) \tag{2}$$

with respect to the coordinates of the spacecraft (X,Y,Z). The two distances in equation 2 are equal to

$$\begin{aligned} R_1^2 &= (X+\mu)^2 + Y^2 + Z^2 \\ R_2^2 &= (X-1+\mu)^2 + Y^2 + Z^2 \end{aligned} \tag{3}$$

and μ is the mass parameter of the three-body system. The only integral of motion available for the system of equations 1 is the Jacobi constant

$$C = 2\Omega(X,Y,Z) - (\dot{X}^2 + \dot{Y}^2 + \dot{Z}^2) \tag{4}$$

and represents a 5-dimensional manifold for the states of the problem within the 6-dimensional phase space. Once a set of initial conditions is given, the Jacobi constant, through equation 4, defines the forbidden and allowed regions of motion

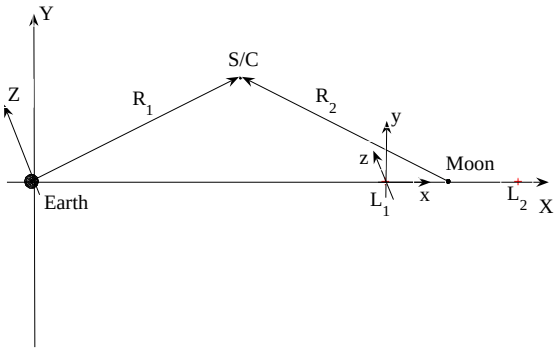

Figure 3: Synodic (X, Y, Z) and L_1-centered (x, y, z) reference frames.

bounded by the Hill's surfaces. The relation between the spacecraft's energy and the Jacobi constant is $C = -2E$ and states that a high value of C is associated to a low energy level. For high values of C the spacecraft is bounded to orbit one of the two primaries; as the value of C is decreased, the forbidden regions open at L_1 and the spacecraft could leave one primary to reach a region close to the other.

Differential system 1 presents five equilibria: the three points L_1, L_2 and L_3 are aligned with the primaries and called collinear (figure 3); the L_4 and L_5 points are at the vertex of two equilateral triangles with the primaries and are called triangular. The present study analyzes the L_1 transit orbits defined within energy levels corresponding to $C_2 < C < C_1$, where C_i denotes the value of the Jacobi constant associated to the i-th libration point $(i = 1, ..., 5)$.

Equations 1 are written in dimensionless units which set the sum of the masses of the primaries, their distance and their angular velocity to one. The following constants have been assumed in this study:

- $\mu = 0.0121506683$, Earth-Moon mass parameter ;
- $l = 384405\ km$, Earth-Moon distance ;
- $T = 27.32\ days$, Earth-Moon period.

With these constants, the unit of length is equal to l, the unit of time is $t = 4.34\ days$ and the unit of speed is $v = 1023.2\ m/s$.

It should be noted that the minimum Δv-cost necessary to carry out an Earth-Moon transfer can be computed by equation 4. In fact, given an initial Earth orbit, a generic point belonging to it has coordinates $\mathbf{x_0} = \{\mathbf{r_0}, \mathbf{v_0}\}^T$ with the associated Jacobi constant equal to $C_0 = 2\Omega(\mathbf{r_0}) - v_0^2$. The Δv, provided parallel to the velocity in order to maximize the variation of the Jacobi constant, must be such that the new velocity $v_0' = v_0 + \Delta v$ defines a Jacobi constant $C_0' = 2\Omega(\mathbf{r_0}) - v_0'^2$ less or equal to $C_1 = 2\Omega(L_1)$. Hence, setting $C_0' = C_1$, the minimum theoretical cost is given by the only positive root of

$$\Delta v^2 + 2v_0\Delta v + C_1 - C_0 = 0\ . \tag{5}$$

Sweetser [6] quantified the lowest Δv necessary to transfer a spacecraft from a

$h_E = 167\ km$ to a $h_M = 100\ km$ Earth and Moon circular orbits. Such *minimum theoretical* Δv is $\Delta v_{th} = \Delta v_{th,e} + \Delta v_{th,m} = 3726\ m/s = 3099\ m/s + 627\ m/s$.

2.1 Linearization around L_1

If l_1 denotes the X-coordinate of the L_1 point and $d = 1 - \mu - l_1$ is the L_1-Moon distance, the (x, y, z) reference frame (figure 3), with origin at L_1 and scaled lengths, can be introduced with the following change of coordinates:

$$x = \frac{X - l_1}{d}\ , \qquad y = \frac{Y}{d}\ , \qquad z = \frac{Z}{d}\ . \tag{6}$$

In these new variables the nonlinear terms of system 1 can be expanded and the resulting linearized equations are [14]

$$\begin{cases} \ddot{x} - 2\dot{y} - (1 + 2c_2)x &= 0 \\ \ddot{y} + 2\dot{x} + (c_2 - 1)y &= 0 \\ \ddot{z} + c_2 z &= 0 \end{cases} \tag{7}$$

where c_2 is a constant depending just on μ as follows:

$$c_2 = \frac{\mu}{(1 - \mu - l_1)^3} + \frac{1 - \mu}{(\mu + l_1)^3}\ . \tag{8}$$

System 7 can be solved analytically with the solution equal to [15]

$$\begin{cases} x(t) &= A_1 e^{\lambda t} + A_2 e^{-\lambda t} + A_3 \cos\omega t + A_4 \sin\omega t \\ y(t) &= -k_1 A_1 e^{\lambda t} + k_1 A_2 e^{-\lambda t} - k_2 A_3 \sin\omega t + k_2 A_4 \cos\omega t \\ z(t) &= A_5 \cos\nu t + A_6 \sin\nu t \end{cases} \tag{9}$$

where A_i $(i = 1, ..., 6)$ are arbitrary amplitudes characterizing the dynamical behavior of the corresponding orbits. The three eigenvalues are equal to

$$\lambda = \sqrt{\frac{c_2 - 2 + \sqrt{9c_2^2 - 8c_2}}{2}}\ , \quad \omega = \sqrt{\frac{2 - c_2 + \sqrt{9c_2^2 - 8c_2}}{2}}\ , \quad \nu = \sqrt{c_2} \tag{10}$$

while the two constants k_1 and k_2 are

$$k_1 = \frac{2c_2 + 1 - \lambda^2}{2\lambda}\ , \qquad k_2 = \frac{2c_2 + 1 + \omega^2}{2\omega}\ . \tag{11}$$

The linear solution can be rewritten by looking at the oscillatory part as having an amplitude and a phase as

$$\begin{cases} x(t) &= A_1 e^{\lambda t} + A_2 e^{-\lambda t} + A_x \cos(\omega t + \varphi) \\ y(t) &= -k_1 A_1 e^{\lambda t} + k_1 A_2 e^{-\lambda t} - k_2 A_x \sin(\omega t + \varphi) \\ z(t) &= A_z \cos(\nu t + \psi) \end{cases} \tag{12}$$

by setting $A_3 = A_x \cos\varphi$, $A_4 = -A_x \sin\varphi$, $A_5 = A_z \cos\psi$ and $A_6 = -A_z \sin\psi$.

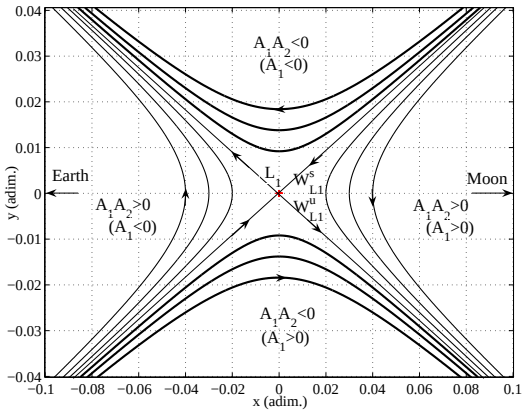

Figure 4: Hyperbolic linear non-transit (solid) and transit (bold) orbits about L_1.

2.2 Linear Transit Orbits through L_1

System 12 clearly shows how the solutions of the nonlinear R3BP behave in the neighborhood of L_1. On the other hand, different choices of amplitudes A_1, A_2, A_x and A_z generate several kinds of solutions. Lyapunov periodic orbits, respectively planar and vertical, can be generated by setting $A_x \neq 0$ and $A_1 = A_2 = A_z = 0$ or $A_z \neq 0$ and $A_1 = A_2 = A_x = 0$. These two orbits have a different period, hence setting $A_x \neq 0$, $A_z \neq 0$ and $A_1 = A_2 = 0$ linear Lissajous orbits can be produced[15].

Much more different is the phase portrait if the stable and unstable amplitudes, A_2 and A_1 respectively, are set to non-trivial values while holding $A_x = A_z = 0$. An initial condition equal to $A_1 \neq 0$ and $A_2 = 0$ generates the L_1 unstable manifold $W^u_{L_1}$; on the contrary, $A_2 \neq 0$ and $A_1 = 0$ gives rise to the L_1 stable manifold $W^s_{L_1}$. Any other non-trivial initial condition generates hyperbolic orbits (figure 4). Conley [5] demonstrated that orbits with $A_1 A_2 < 0$ are *transit* hyperbolic orbits and are the only ones able to link the Earth's and the Moon's neighborhoods. Such orbits shadow the L_1 invariant manifolds as their amplitudes decrease. Thus, the generic planar transit orbit can be described by

$$\begin{cases} x(t) &= A_1 e^{\lambda t} + A_2 e^{-\lambda t} \\ y(t) &= -k_1 A_1 e^{\lambda t} + k_1 A_2 e^{-\lambda t} \\ z(t) &= 0 \end{cases} \tag{13}$$

leaving two parameters free for its computation.

2.3 Nonlinear Transit Orbits through L_1

Since this works aims at computing low energy Earth-to-Moon transfers flowing on transit orbits, it is convenient to find an initial condition which generates such orbits under the full nonlinear system 1. In other words, system 13 must be used to generate initial conditions associated to transit orbits and parameterized with just

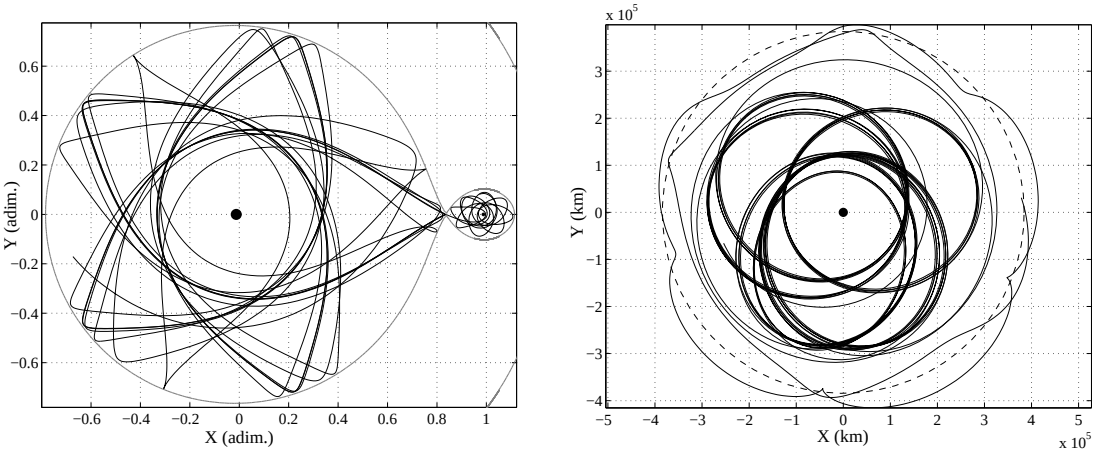

(a) Synodic frame. (b) Earth-centered frame.

Figure 5: A L_1 nonlinear transit orbit ($A_1 = 0.01$).

one amplitude. For $t = 0$, system 13 becomes

$$\begin{cases} x(0) &= A_1 + A_2 \\ y(0) &= k_1(A_2 - A_1) \\ z(0) &= 0 \end{cases} \tag{14}$$

and forcing the hyperbolae to intersect the plane $x = 0$ when $t = 0$ results in $A_2 = -A_1$. In this way the amplitude-depending initial condition for the generation of the transit orbits is $\mathbf{x_0}(A_1) = \{0, -2k_1A_1, 0, 2\lambda A_1, 0, 0\}^T$. Now, rewriting this expression in R3BP original coordinates, one gets an initial condition to propagate within system 1:

$$\mathbf{X_0}(A_1) = d\mathbf{x_0}(A_1) + \{l_1, 0, 0, 0, 0, 0\}^T \tag{15}$$

where constants correspond to those introduced in the previous section.

A family of planar nonlinear transit orbits can be computed by integrating initial condition 15 under the system 1 in the same way as the computation of the invariant manifolds involves the integration of appropriate initial conditions given by the linear analysis (figure 5). Amplitudes greater than zero are associated to Earth-to-Moon transit orbits, while values of A_1 less than zero generate symmetric Moon-to-Earth transit orbits (figure 4). In fact, it is convenient to note that system 1 is invariant under the following change of coordinates:

$$S: \ (X, Y, Z, \dot{X}, \dot{Y}, \dot{Z}, t) \ \rightarrow \ (X, -Y, Z, -\dot{X}, \dot{Y}, -\dot{Z}, -t) \ . \tag{16}$$

Thus, the L_1-Moon leg of the transit orbit can be obtained by forward integrating the initial condition 15, while the Earth-L_1 leg can be computed either by integrating backward in time the same initial condition or by forward propagating the symmetric initial condition $\mathbf{X}(-A_1)$ and then applying the symmetry S. This is the reason why throughout the paper we refer at this leg as the L_1-Earth leg instead of the

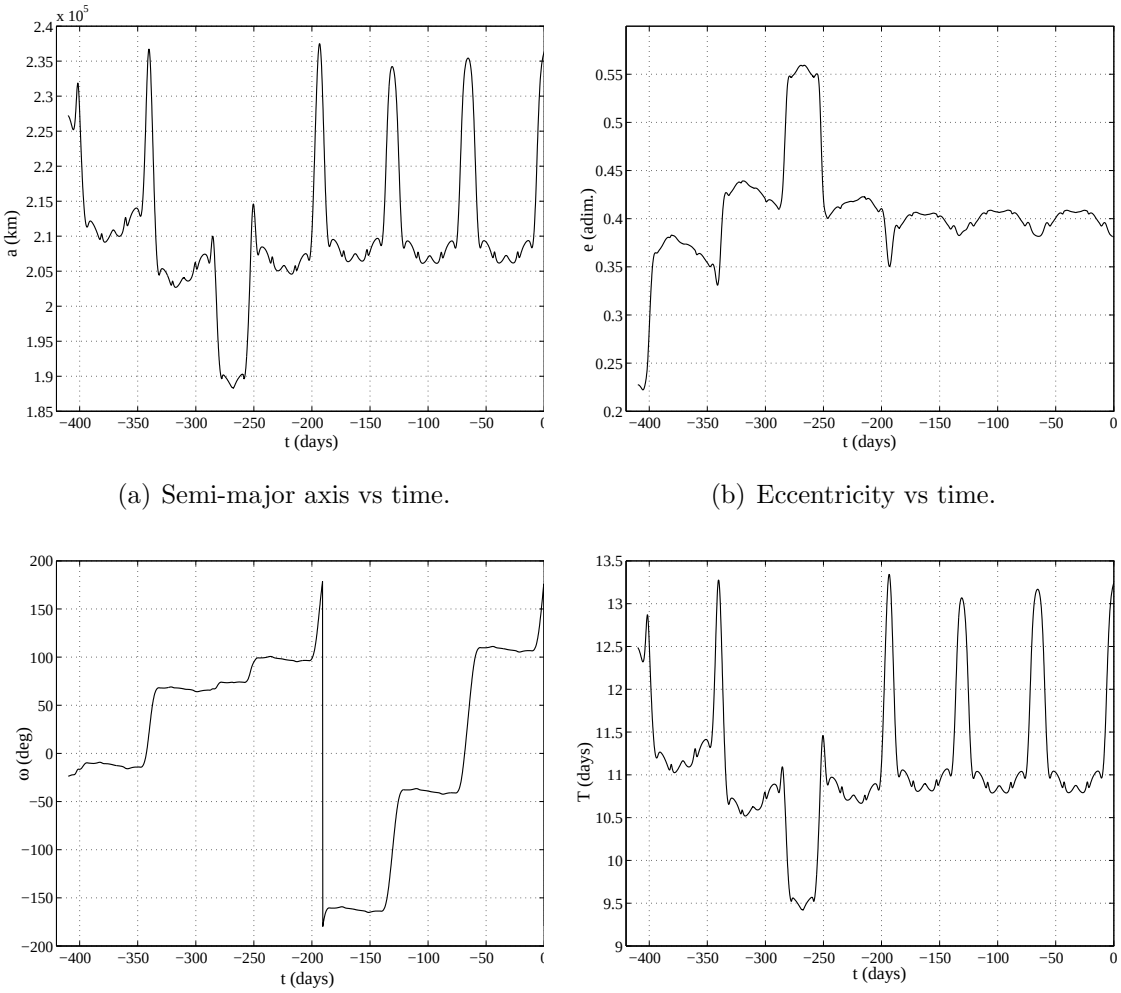

(a) Semi-major axis vs time.

(b) Eccentricity vs time.

(c) Perigee anomaly vs time.

(d) Period vs time.

Figure 6: Orbital elements associated to the L_1-Earth leg of the trajectory in figure 5.

Earth-L_1 leg. Hence, by this parametrization, the design of the whole transfer path is divided in two: the L_1-Moon (L_1-M) and the L_1-Earth (L_1-E) legs. Figure 5 shows a nonlinear transit with $A_1 = 0.01$ whose L_1-M leg is propagated for 4π adimensional time units (54.6 *days*) while the L_1-E is 30π units long (409.8 *days*). Figure 5(a) and 5(b) shows respectively the orbit viewed in the synodic and Earth-centered frames. Several observations should be made on the orbit of figure 5.

First, the trajectory, in a short time, does not reach the Earth's neighborhood and so does not allow a *direct* injection starting from a low altitude Earth orbit. This helps to understand why previously cited works [10], [11], [12] and [13] were able to find very low energy transfers just between high altitude Earth and Moon orbits. On the contrary, in order to link low altitude orbits, as in [1] and [7], additional mid-course maneuvers will be required. The strategy on how to execute such maneuvers is given in the next section.

Second, as observed in [7], the L_1-E leg is a trajectory close to a 5:2 resonant orbit with the Moon. Resonances occur when the line of apsides is close to the Earth-

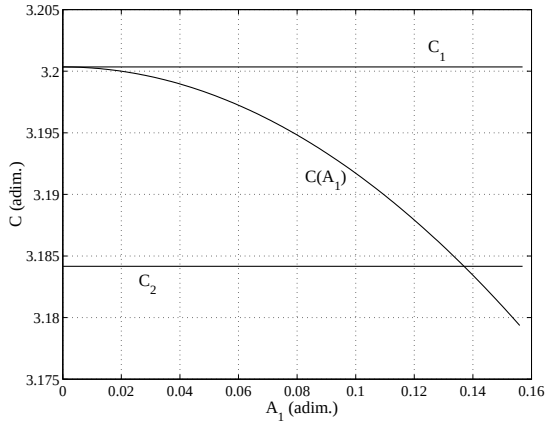

Figure 7: $C = C(A_1)$ profile and its intersection with C_2.

Moon line (i.e. X-axis in the synodic frame) and produce an apocenter/pericenter raising; in other words, the spacecraft, when orbiting the Earth, is "pumped-up" by the Moon's gravitational attraction. Resonances in the L_1-E leg are clearly visible in figure 6 where the time history (obtained by backward time propagation) of the most important orbital elements is shown. The orbits overlap for five times every two Moon revolutions; then semi-major axis, eccentricity, pericenter anomaly and period swiftly change and remain roughly constant for other 55 days.

Third, initial conditions are obtained through 15, but the higher is A_1 the lower is the Jacobi constant C according to equation 4. Hence, there exist a relation $C(A_1) = C(\mathbf{X}(A_1))$ and there will be a critical value of amplitude $A_1 = \bar{A_1}$ such that $C(\bar{A_1}) = C_2$. With amplitudes grater than $\bar{A_1}$ the Hill's region opens at L_2 and so the transit orbit is no more bounded to orbit the Moon being free to leave it from the far side. This is the reason why the transit orbits dealt with in the present work have amplitudes $A_1 < \bar{A_1}$. Figure 7 shows the $C = C(A_1)$ profile and its intersection with the $C = C_2$ level which determines the value of the critical amplitude. This value has been calculated equal to $\bar{A_1} = 0.136960$.

3 Design Method

In previous works [7], [10]-[13] trajectories defined in the R3BP have been obtained by forward integration of perturbed initial conditions corresponding to Δv's given at departure until the L_1 neighborhood was reached; but the point is that, as observed in [8], the problem so stated is very sentive to small variations in the initial conditions.

This paper aims at designing Earth-to-Moon trajectories which use nonlinear transit orbits and their dynamical features to lower the Δv cost and so the propellant mass fraction of a mission to the Moon. In this way the simultaneous presence of the Earth and the Moon is *embedded* in the design process. In fact, when the spacecraft orbits the Earth, the presence of the Moon is not ignored, as in the traditional preliminary design methods, but its gravitational attraction is exploited to change the orbital elements since the spacecraft is placed on a resonant orbit with the

Moon. Unfortunately such orbits, in a short time, do not get close to low Earth orbits and so additional maneuvers are required to perform the link between the departure orbits and the nonlinear transit orbits. Furthermore, after the transit, other maneuvers are needed to break the chaotic motion in order to stabilize the spacecraft in low lunar orbits. The tool developed to carry out these maneuvers has been called Lambert's three-body arc and represents an extension of the most common Lambert's two-body arc.

3.1 Lambert's Three-Body Arc

The Lambert's problem consists in finding the conic path linking two given points in a given time. Equivalently, the Lambert's three-body arc links two given points, in a given time, within the R3BP dynamics stated by system of equations 1. Let $\mathbf{x_1} = \{\mathbf{r_1}, \mathbf{v_1}\}^T$ and $\mathbf{x_2} = \{\mathbf{r_2}, \mathbf{v_2}\}^T$ be two points in the phase space and let Δt be a time interval. The goal is to find an orbit $\mathbf{x} = \mathbf{x}(t) = \{\mathbf{r}(t), \mathbf{v}(t)\}^T$ satisfying the 2PBVP given by the two end-point conditions $\mathbf{r}(t_0) = \mathbf{r_1}$ and $\mathbf{r}(t_0 + \Delta t) = \mathbf{r_2}$. In other words, one has to find a new initial condition (i.e. a new velocity)

$$\mathbf{x_1^+} = \{\mathbf{r_1}, \mathbf{v_1^+}\}^T \tag{17}$$

such that

$$\varphi(\mathbf{x_1^+}, \Delta t) = \mathbf{x_2^-} \tag{18}$$

where

$$\mathbf{x_2^-} = \{\mathbf{r_2}, \mathbf{v_2^-}\}^T \tag{19}$$

and $\varphi(\mathbf{x}, t)$ represents the flow, under system 1, of the initial condition $\mathbf{x}$ after the time t. The cost necessary to perform such a step is defined as $\Delta v = \|\mathbf{v_1^+} - \mathbf{v_1}\| + \|\mathbf{v_2} - \mathbf{v_2^-}\|$ and will be used in the next sections to evaluate the performances of a generic solution. The 2PBVP stated above has been solved using a direct transcription method which employs a Hermite-Simpson fourth-order variable-step discretization scheme and a Newton solver [16].

3.2 Design Strategy

The design strategy is summarized as follows:

1. Fix an initial amplitude A_1 and get its associated initial condition $\mathbf{X_0}(A_1)$ through relation 15 ;
2. Flow the nonlinear transit orbit with the method shown in section 2.3 until the Earth and Moon neighborhoods are reached;
3. Choose a low Earth and a low Moon orbit with altitude respectively equal to h_E and h_M;
4. Link a point on the Earth orbit with the transit trajectory by means of a Lambert' arc;
5. Link a point on the Moon orbit with the transit trajectory using another Lambert's arc.

Figure 8 illustrates a sketch of the described method together with the two main building blocks whose details will be described in the next two sections.

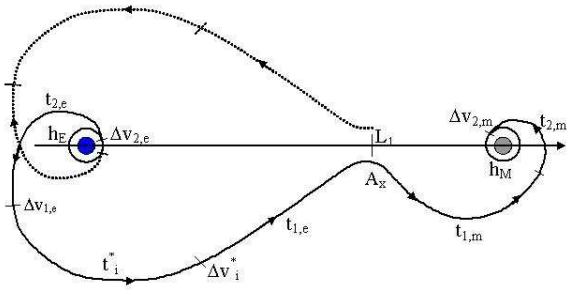

Figure 8: A concept sketch showing the design strategy.

3.2.1 L_1-Moon Leg

Let $\mathbf{X_0}(A_1)$ be the initial condition stated by equation 15 and let $\mathbf{X_1^-} = \varphi(\mathbf{X_0}, t_{1,m}) = \{\mathbf{r_1}, \mathbf{v_1^-}\}^T$ be a point on the nonlinear transit orbit parameterized by the time $t_{1,m}$. The L_1-M leg aims at linking the transit orbit with a low Moon orbit with altitude h_M. Let $\mathbf{X_2^+}(\theta_m) = \{\mathbf{r_2}, \mathbf{v_2^+}\}^T$ be a point belonging to such Moon circular orbit with $\|\mathbf{v_2^+} + \mathbf{k} \times \mathbf{r_2}\| = \sqrt{k_M/(R_M + h_M)}$ where k_M and R_M are respectively the gravitational constant and the radius of the Moon, $\mathbf{k}$ is the unity angular velocity vector and θ_m is the anomaly along the circular orbit. Now, in analogy with section 3.1, the task is to solve the 2PBVP between the two configuration vectors $\mathbf{r_1}$ and $\mathbf{r_2}$ within a time interval identified by another parameter equal to $t_{2,m}$. When the problem is solved one has the new initial condition $\mathbf{X_1^+} = \{\mathbf{r_1}, \mathbf{v_1^+}\}^T$ such that $\varphi(\mathbf{X_1^+}, t_{2,m}) = \{\mathbf{r_2}, \mathbf{v_2^-}\}^T$. Whit this solution in hand, the cost of the L_1-M leg can be evaluated as

$$\Delta v_m(t_{1,m}, t_{2,m}, \theta_m) = \Delta v_{1,m} + \Delta v_{2,m} = \|\mathbf{v_1^+} - \mathbf{v_1^-}\| + \|\mathbf{v_2^+} - \mathbf{v_2^-}\| \tag{20}$$

while its associated time of flight is equal to

$$\Delta t_m = t_{1,m} + t_{2,m} \ . \tag{21}$$

Both the 2PBVP and the initial value problems arising in this context have been solved with absolute and relative tolerances equal to 10^{-8}. These values are smaller than the ones usually found in literature relative to astrodynamics integrations, but one should remember that here the preliminary trajectory design is dealt with a simplified model and even greater perturbations arise when more precise models are introduced.

Figure 9 shows an example of the L_1-M leg viewed in both the synodic (figure 9(a)) and Moon-centered (figure 9(b)) frames. The '+' markers in the synodic frame indicate the bounds of the Lambert's three-body arc which correspond to the maneuver points. In this case a very small intermediate Δv maneuver (first marker) has been introduced to lower to total cost of this leg.

3.2.2 L_1-Earth Leg

The design of the L_1-E leg follows directly from the L_1-M leg but it is much more difficult than the previous one because this time the Lambert's three-body problem is hard to solve between a point on the low Earth orbit and, typically, the apocenter of the L_1 transit orbit.

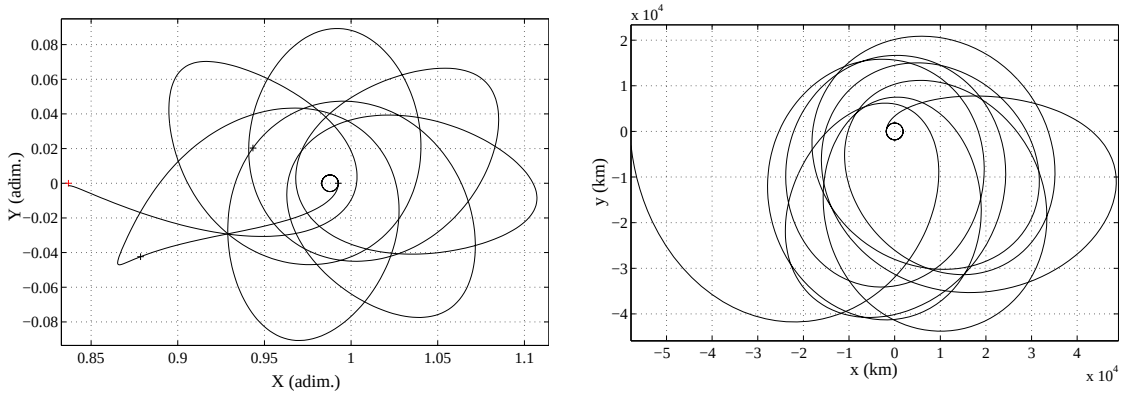

(a) Synodic frame.

(b) Moon-centered frame.

Figure 9: An example of the L_1-Moon leg.

This feature is probably due to the high time associated to the solution linking the two end-points of the problem. A way to overcome this drawback is the introduction of very small Δv maneuvers which perturbate and slightly change the shape of the transit orbit making the 2PBVP able to converge. The time and the size of the n small maneuvers has been left free.

Hence, if $\mathbf{X_1^-} = \varphi(\mathbf{X_0}, t_{1,e}) = \{\mathbf{r_1}, \mathbf{v_1^-}\}^T$ is a point on the transit orbit, parameterized by the time $t_{1,e}$, the state after the first maneuver will be $\mathbf{X_1^+} = \{\mathbf{r_1}, \mathbf{v_1^+}\}^T$ with the size Δv_1^* chosen parallel to the velocity in order to maximize the variation of the Jacobi constant

$$\mathbf{v_1^+} = \mathbf{v_1^-} + \Delta v_1^* \frac{\mathbf{v_1^-}}{v_1^-} \ . \tag{22}$$

The point $\mathbf{X_1^+}$ can be propagated for a time equal to t_1^* which identifies another point $\mathbf{X_2^-} = \varphi(\mathbf{X_1^+}, t_1^*)$. Now, another small maneuver is carried out in the same way as the previous. This process goes on until the last point $\mathbf{X_n^-} = \{\mathbf{r_n}, \mathbf{v_n^-}\}^T$ is linked with a point on the h_E circular Earth orbit with states $\mathbf{X_{n+1}^+}(\theta_e) = \{\mathbf{r_{n+1}}, \mathbf{v_{n+1}^+}\}^T$ with again $\|\mathbf{v_{n+1}^+} + \mathbf{k} \times \mathbf{r_{n+1}}\| = \sqrt{k_E/(h_E + R_E)}$ and θ_e the anomaly along the parking orbit. Solving this second 2PBVP means having the state $\mathbf{X_n^+} = \{\mathbf{r_n}, \mathbf{v_n^+}\}^T$ such that $\varphi(\mathbf{X_n^+}, t_{2,e}) = \{\mathbf{r_{n+1}}, \mathbf{v_{n+1}^-}\}^T$ and its cost is $\Delta v_{1,e} + \Delta v_{2,e} = \|\mathbf{v_n^+} - \mathbf{v_n^-}\| + \|\mathbf{v_{n+1}^+} - \mathbf{v_{n+1}^-}\|$.

At the end of this process, the cost and the time of flight of the L_1-Earth solution can be evaluated as

$$\Delta v_e(t_i^*, \Delta v_i^*, t_{1,e}, t_{2,e}, \theta_e) = \sum_{i=1}^{n} \Delta v_i^* + \Delta v_{1,e} + \Delta v_{2,e} \tag{23}$$

and

$$\Delta t_e = \sum_{i=1}^{n} t_i^* + t_{1,e} + t_{2,e} \ . \tag{24}$$

Figure 10 shows a typical L_1-Earth leg as viewed in both the synodic and Earth-centered reference frames.

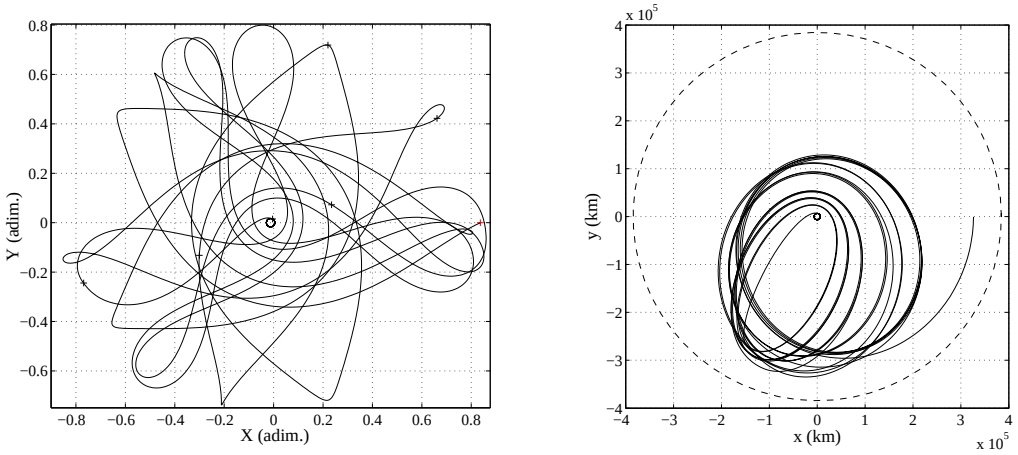

(a) Synodic frame. (b) Earth-centered frame.

Figure 10: An example of the L_1-Earth leg.

3.2.3 Patched trajectory

Once the two legs have been designed independently, the whole Earth-to-Moon trajectory can be obtained by patching them together. It is straightforward that just legs parameterized with the same A_1 amplitude can be patched together because only in this case the continuity is assured at the patching point $\mathbf{X_0}(A_1)$. It should be observed that this approach splits the whole problem into two different subproblems, each having a reduced number of variables. The two legs can be optimized independently and then joined again for the definition of the whole Earth-to-Moon path.

The total cost and the time required to the Earth-Moon transfers can be evaluated directly adding equation 20 to equation 23 and equation 21 to equation 24:

$$\begin{cases} \Delta v &= \Delta v_m + \Delta v_e \\ \Delta t &= \Delta t_m + \Delta t_e \end{cases} \tag{25}$$

4 Results

This section summarizes the set of results found for the two legs and so the for the whole Earth-to-Moon transfers. Table 1 shows some sample solutions found for the L_1-Moon case, while figure 11(a) illustrates the whole family of solutions from the Δv_m vs Δt_m standpoint. The best solution found, corresponding to the amplitude $A_1 = 0.01$, has $\Delta v_m = 629.9\ m/s$ and $\Delta t_m = 40.7\ days$ meaning that the minimum theoretical Δv for the L_1-M leg, $\Delta v_{th,m} = 627\ m/s$, has been almost reached. This means that the L_1-Moon problem, as stated in the previous sections, reveals very efficient and solutions very close to the minimum theoretical one appear.

The case of L_1-Earth trajectories is much more different. The number of variables defining this legs is higher because the intermediate low Δv maneuvers require two additional variables each: Δv_i^* and t_i^*. Hence, with just four maneuvers, the additional number of variables is equal to eight. Taking into account the time of the Lambert's arc, the time of the transit orbit and the anomaly along the Earth circular orbit, the total number of variables for the L_1-Earth leg is eleven. Furthermore, it seems that the structure of the L_1 transit orbit must be *broken* in order to find low energy solutions: this is because a direct injection from the circular to the transit orbit is very expensive, so the intermediate

$A_1 = 0.001$		$A_1 = 0.01$		$A_1 = 0.1$	
Δv_m (m/s)	Δt_m $(days)$	Δv_m (m/s)	Δt_m $(days)$	Δv_m (m/s)	Δt_m $(days)$
645.9	42.9	**629.9**	**40.7**	**634.9**	**49.5**
686.7	46.0	631.4	40.4	658.5	23.2
707.0	9.3	638.2	43.4	705.1	2.9

Table 1: Sample results for the L_1-Moon leg (the best ones in bold).

$A_1 = 0.001$		$A_1 = 0.01$		$A_1 = 0.1$	
Δv_e (m/s)	Δt_e $(days)$	Δv_e (m/s)	Δt_e $(days)$	Δv_e (m/s)	Δt_e $(days)$
3335.8	208.0	**3265.0**	**214.8**	**3265.1**	**144.2**
3372.0	209.3	3289.5	214.6	3277.8	144.1
3378.2	208.9	3301.4	145.9	3283.2	178.3

Table 2: Sample results for the L_1-Earth leg (the best ones in bold).

maneuvers lower this cost but, at the same time, move away the energy of the solution from the minimum.

The first sample solution, corresponding to $A_1 = 0.1$, has $\Delta v_e = 3265.1\ m/s$ and $\Delta t_e = 144.2\ days$ and, combined with the cheaper L_1-Moon solution having the same amplitude, makes $\Delta v = 3900\ m/s$ and $\Delta t = 193.7\ days$. Figure 12 shows this solution where, after departure, the spacecraft makes several close Earth passages and, from a patched-conic point of view, three Moon swing-by's. After the L_1 passage, a very small maneuver is used

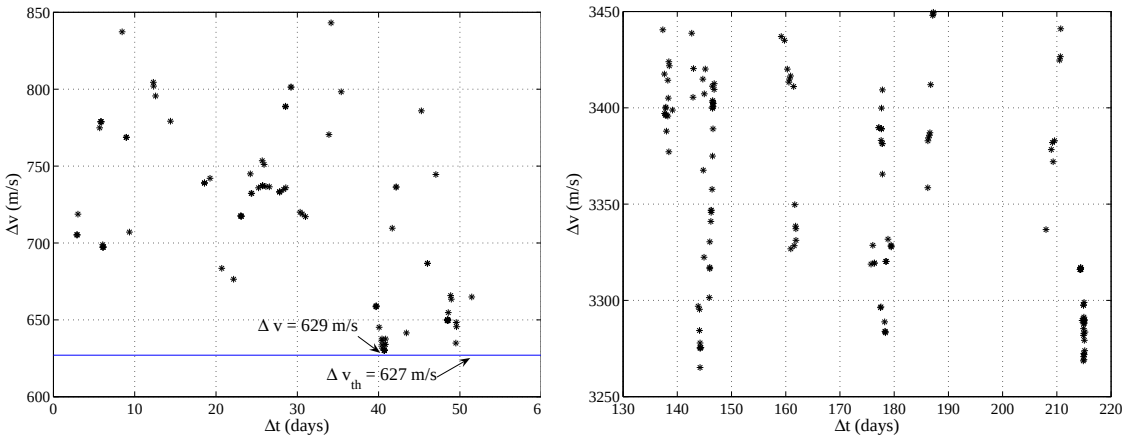

(a) L_1-Moon leg. (b) L_1-Earth leg.

Figure 11: Set of results found for both legs.

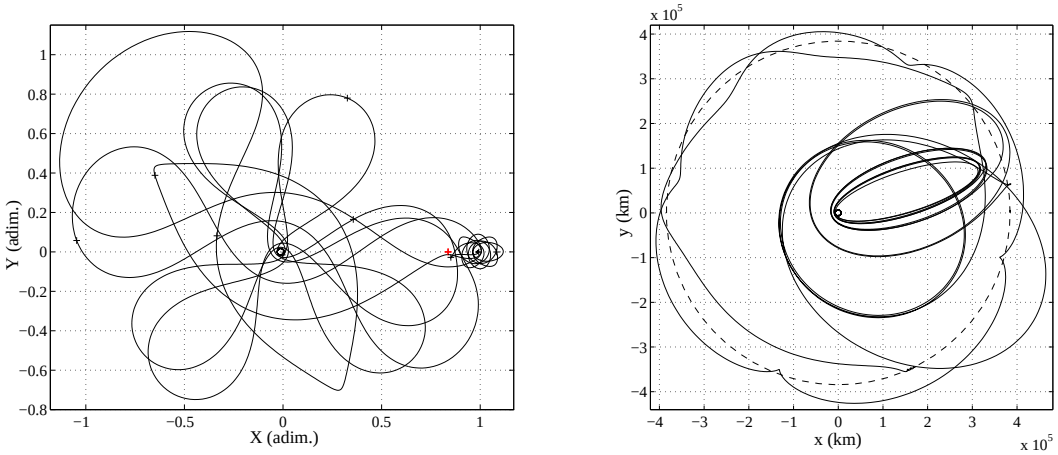

(a) Synodic frame. (b) Earth-centered frame.

Figure 12: Earth-Moon transfer with $\Delta v = 3900\ m/s$ and $\Delta t = 193.7\ days$.

to adjust the transit orbit which is then linked with the low Moon orbit. The second sample solution is defined by adding the bold rows in tables 1 and 2 corresponding to $A_1 = 0.01$. This solution, represented in figure 13, has $\Delta v = 3894.9\ m/s$ and is $\Delta t = 255.5\ days$ long. This time the spacecraft is bounded within the Moon's orbit and combines small Δv maneuvers and Moon resonances to raise its perigee and apogee. The reader should remind that, as mentioned in section 1, a classical Hohmann transfer to the Moon requires a cost equal to $\Delta v_H = 3991\ m/s$ [1].

Figures 12 and 13 highlights how cheap transfers present a number of close Earth passage. This feature makes even more difficult to find an acceptable solution since Earth impact trajectories, to be avoided, can appear by slightly changing the size of the intermediate Δv.

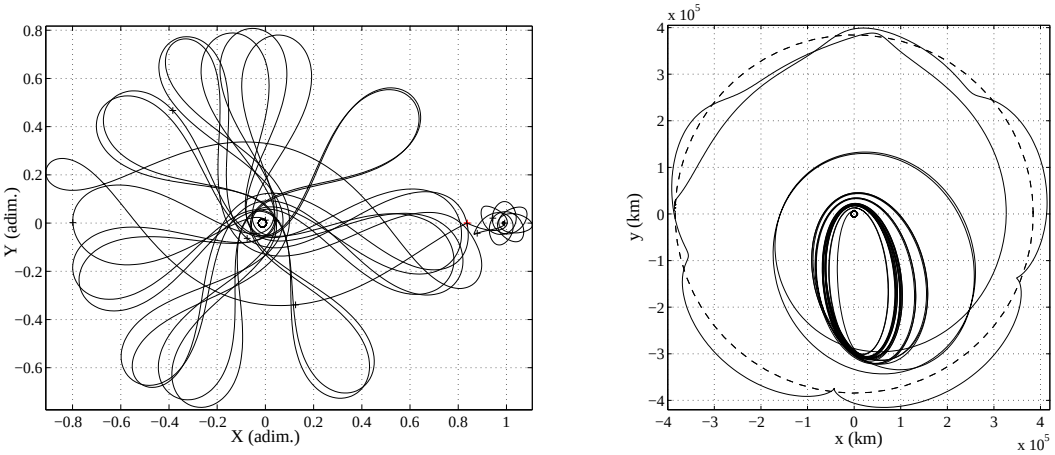

(a) Synodic frame. (b) Earth-centered frame.

Figure 13: Earth-Moon transfer with $\Delta v = 3894.9\ m/s$ and $\Delta t = 255.5\ days$.

5 Conclusions

In this study the design of low energy Earth-to-Moon transfers, exploiting the L_1 hyperbolic dynamics, has been faced within the frame of the circular restricted three-body problem. A family of solutions has been found which aims at approaching the Moon from the Earth-side.

The problem, as stated in section 3, reveals very efficient when L_1-Moon solutions are desired. In such a context, indeed, a number of solutions close to the minimum theoretical one have been found: the best is $\Delta v_m = 629.9\ m/s$ while the minimum is $\Delta v_{th,m} = 627\ m/s$ [6]. On the contrary, solutions concerning the L_1-Earth arc do not seem to approach their minimum because the best one ($\Delta v_e = 3265.0\ m/s$) is quite far from $\Delta v_{th,e} = 3100\ m/s$. Nevertheless, the best Δv vs Δt solution found allows to save approximately 100 m/s with respect to the Hohmann transfer but requires 193 *days* to reach the Moon. It could be that cheaper solutions appear for longer times of flight, but in the present study just solutions shorter than 300 *days* have been searched for. Solutions found here could be very appropriate paths for such missions, as lunar cargos, where the maximization of the payload mass is required without any particular constraint on the time of flight.

Since the transit orbits have been assessed here to be an interesting tool for the Moon orbit insertion, a further step will concern the use of the L_1 hyperbolic dynamics combined with low thrust propulsion. In this way, a trust arc could be used to target a piece of L_1 transit orbit in analogy to the Lambert's three-body arc used in this study. Furthermore, the effect of the fourth-body perturbations (e.g. the Sun in this case) on the designed trajectories should be assessed.

Acknowledgments

Part of the work presented in this paper has been carried out at Politecnico di Milano, under ESA/ESTEC contract No. 18147/04/NL/MV, in the frame of the Ariadna context [17].

References

[1] E.A. Belbruno and J.K. Miller – *Sun-Perturbated Earth-to-Moon Transfers with Ballistic Capture* – Journal of Guidance, Control and Dynamics, Vol. 16, No. 4, pp. 770-775, 1993

[2] L.A. D'Amario and T. N. Edelbaum – *Minimum Impulse Three-Body Trajectories* – AIAA Journal, Vol. 12, No. 4, pp. 455-462, 1974

[3] C.L. Pu and T.N. Edelbaum – *Four-Body Trajectory Optimization* – AIAA Journal, Vol. 13, No. 3, pp. 333-336, 1975

[4] W.S. Koon, M.W. Lo, J.E. Marsden and S.D. Ross – *Low Energy Transfer to the Moon* – Celestial Mechanics and Dynamical Astronomy, Vol. 81, No. 1, pp. 63-73, 2001

[5] C.C. Conley – *Low Energy Transit Orbits in the Restricted Three-Body Problem* – SIAM Journal of Applied Mathematics, Vol. 16, No. 4, pp. 732-746, 1968

[6] T.H. Sweetser – *An Estimate of the Global Minimum Δv needed for Earth-Moon Transfer* – Advances in the Astronautical Sciences Series, Vol. 75, No. 1, pp. 111-120, 1991

[7] H.J. Pernicka, D.P. Scarberry, S.M. Marsh and T.H. Sweetser – *A Search for Low Δv Earth-to-Moon Trajectories* – The Journal of the Astronautical Sciences, Vol. 43, No. 1, pp. 77-88, 1995

[8] G. Mengali and A. Quarta – *Optimization of Biimpulsive Trajectories in the Earth-Moon Restricted Three-Body System* – Journal of Guidance, Control and Dynamics, Vol. 28, No. 2, pp. 209-216, 2005

[9] K. Yagasaki – *Sun-Perturbated Earth-to-Moon Transfers with Low Energy and Moderate Flight Time* – Celestial Mechanics and Dynamical Astronomy, Vol. 90, pp. 197-212, 2004

[10] E.M. Bolt and J.D. Meiss – *Targeting Chaotic Orbits to the Moon Through Recurrence* — Physics Letters A 204, pp. 373-378, 1995

[11] C.G. Schroer and E. Ott – *Targeting in Hamiltonian Systems that have a Mixed Regular/Chaotic Phase Spaces* – Chaos, Vol. 7, No. 4, pp. 512-519, 1997

[12] E.E.N. Macau – *Using Chaos to Guide a Spacecraft to the Moon* – IAF-98-A.3.05, IAC 1998, Melbourne, Australia, Sept. 28 - Oct. 2, 1998

[13] S.D. Ross – *Trade-Off Between Fuel and Time Optimization* – New Trends in Astrodynamics and Application, Princeton University, 20-22 January, 2003

[14] Á. Jorba and J. Masdemont – *Dynamics in the Center Manifold of the Collinear Points of the Restricted Three Body Problem* – Physica D 132, pp. 189-213, 1999

[15] E. Canalias, J. Cobos and J. Masdemont – *Impulsive Transfers between Lissajous Libration Point Orbits* – The Journal of the Astronautical Sciences, Vol. 51, No. 4, pp. 361-390, 2003

[16] L.F. Shampine, J.K. Kierzenka and M.W. Reichelt – *Solving Boundary Value Problems for Ordinary Differential Equations in MATLAB with bvp4c* – www.mathworks.com, October 2000

[17] F. Bernelli-Zazzera, F. Topputo and M. Massari – *Assessment of Mission Design Including Utilization of Libration Points and Weak Stability Boundaries* – Final Report, ESTEC Contract No. 18147/04/NL/MV, June 2004